

Common medial frontal mechanisms of adaptive control in humans and rodents

Nandakumar S Narayanan^{1,5}, James F Cavanagh^{2,5}, Michael J Frank^{2,3} & Mark Laubach⁴

In this report we describe how common brain networks within the medial frontal cortex (MFC) facilitate adaptive behavioral control in rodents and humans. We demonstrate that after errors, low-frequency oscillations below 12 Hz are modulated over the midfrontal cortex in humans and within the prelimbic and anterior cingulate regions of the MFC in rats. These oscillations were phase locked between the MFC and motor areas in both rats and humans. In rats, single neurons that encoded prior behavioral outcomes were phase coherent with low-frequency field oscillations, particularly after errors. Inactivating the medial frontal regions in rats led to impaired behavioral adjustments after errors, eliminated the differential expression of low-frequency oscillations after errors and increased low-frequency spike-field coupling within the motor cortex. Our results describe a new mechanism for behavioral adaptation through low-frequency oscillations and elucidate how medial frontal networks synchronize brain activity to guide performance.

Adaptive control allows an agent to change behavior in order to improve performance after mistakes are made^{1,2}. This process involves guiding behavior according to a previous outcome and is commonly associated with prediction error signaling in medial frontal areas such as the anterior cingulate cortex^{3,4}. Adaptive control is compromised in a number of psychiatric and neurological disorders, such as schizophrenia, attention deficit hyperactivity disorder, obsessive compulsive disorder, Parkinson's disease and schizophrenia^{2,5-7}. However, our understanding of these deficits is hindered by a lack of knowledge of the specific mechanisms by which the MFC adjusts performance on the basis of prior outcome. Here we describe how common features of adaptive control in rodents and humans appear to be mediated by medial frontal low-frequency oscillations. This similarity allowed us to utilize cross-species comparisons to explore candidate mechanistic processes by which medial frontal regions guide behavior.

The MFC has been demonstrated to guide behavior according to behavioral goals⁸⁻¹⁰ and monitor behavioral states^{2,11} in the service of optimal performance^{12,13}. For instance, in reaction-time tasks, participants typically engage in a deliberate speed-accuracy tradeoff if the previous trial was an error, a phenomenon that is known as post-error slowing¹⁴⁻¹⁶. Interestingly, rodents also exhibit post-error slowing after errors¹¹. In both rodents and humans, lesions in the MFC impair such processes^{11,13,17}. A detailed understanding of the specific mechanism by which the MFC improves performance would facilitate the understanding, diagnosis and treatment of diseases that are associated with impaired adaptive control^{18,19}.

In the present study, we recorded from the medial frontal and motor networks in both rodents and humans during a simple time-estimation task. This new cross-species approach allowed us to

characterize a conserved neurobehavioral repertoire across mammalian species and provided mechanistic insight into how medial frontal networks guide behavior in accordance with behavioral goals. We found that rats and humans exhibited similar enhancement of low-frequency oscillations after errors in a time-estimation task and that these neural signals were commonly related to trial-by-trial behavioral adaptation. Most notably, pharmacological disruption of the rodent MFC eliminated the selective expression of post-error low-frequency oscillations in the motor cortex, as well as adaptive post-error behavioral adjustment.

RESULTS

Similar post-error signals in humans and rodents

To examine the relationship between error-related activity in humans and rodents, we recorded neural activity using a time-estimation task (**Fig. 1a**) in which a response was required at an estimated time interval (human, 1.4 s; rat, 1 s) and an imperative stimulus (tone) was presented at the target time in 50% of the trials²⁰. Humans and rodents had comparable response latencies from the target time (236 ± 18 ms (mean \pm s.e.m.) for humans compared to 250 ± 40 ms for rats) but somewhat different premature error rates ($7 \pm 1\%$ for humans compared to $25 \pm 3\%$ for rats).

In 11 humans, we recorded 64-channel scalp electroencephalograms (EEGs) while they performed this task. We then compared event-related potentials (ERPs) in trials after correct responses and after premature error responses (post-correct and post-error trials, respectively; **Fig. 1a**). We measured human ERPs as the difference between the mean of the first major peak (P3: 275 ± 25 ms) and the preceding trough (N1: 125 ± 25 ms), which corresponded to an approximate frequency of 6 Hz. In post-error trials, humans

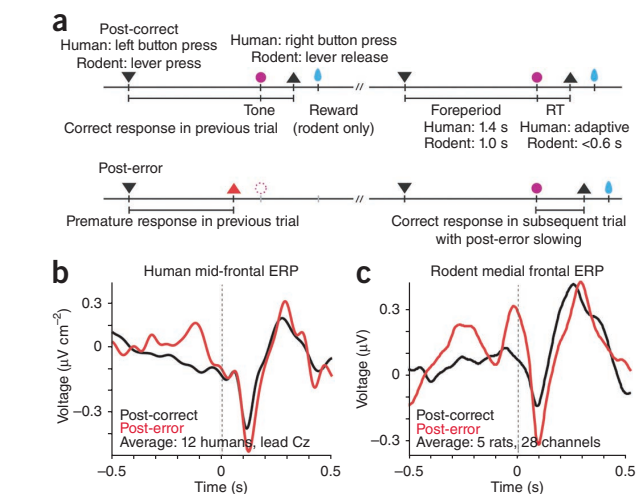
¹Department of Neurology, Carver College of Medicine, The University of Iowa, Iowa City, Iowa, USA. ²Cognitive, Linguistic and Psychological Sciences, Brown University, Providence, Rhode Island, USA. ³Department of Psychiatry and Brown Institute for Brain Science, Brown University, Providence, Rhode Island, USA. ⁴The John B. Pierce Laboratory and Department of Neurobiology, Yale University School of Medicine, New Haven, Connecticut, USA. ⁵These authors contributed equally to this work. Correspondence should be addressed to M.L. (mlaubach@jbpierce.org).

Received 18 July; accepted 29 August; published online 20 October 2013; doi:10.1038/nn.3549

Figure 1 Common mechanisms of medial frontal cortical oscillations during adaptive control in rats and humans. **(a)** Sequence of events in the time-estimation task in post-correct as compared to post-error trials (black). All analyses were restricted to correct trials as a function of prior outcome. The black inverted triangle indicates the lever or button press, the purple circle indicates the tone, the black triangle indicates the button or lever release, and the blue oval indicates the reward (rodent only). Imperative tones occurred at the target time in 50% of trials. RT, response time. **(b)** Average event-related potentials over the midfrontal cortex (electrode Cz) in humans aligned to the target time. Amplitudes were significantly increased in post-error (red) as compared to post-correct (black) trials. **(c)** Rodent medial frontal field potentials were also significantly increased in post-error (red) as compared to post-correct (black) trials; the results were highly similar to those in humans. The data shown are from 28 medial frontal channels in five rats and are aligned to the target time.

had significantly larger midfrontal ERPs to the target time as compared to trials that were preceded by correct responses (paired *t* test $t_{10} = 2.75$, $P < 0.02$; **Fig. 1b**).

We compared these signals to intracortical field potentials recorded from 28 channels in the MFC of five rodents (**Supplementary Fig. 1**). Notably, the intracortical local field potentials in the rodents had a nearly identical pattern to those in humans during the response



period (**Fig. 1c**), with enhanced ERPs in post-error trials compared to in post-correct trials (paired *t* test $t_{27} = 1.90$, $P < 0.04$). These data suggest a common neural mechanism of adaptive control in rodents and humans.

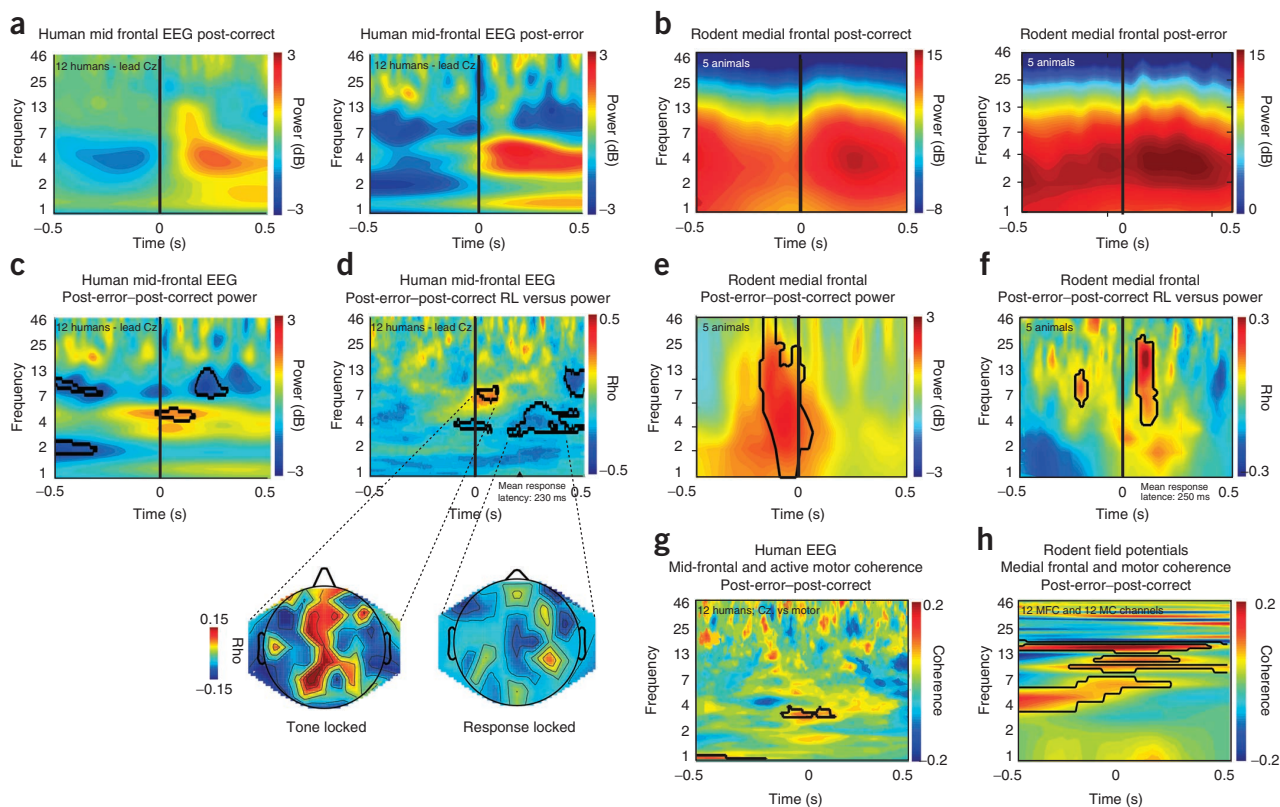
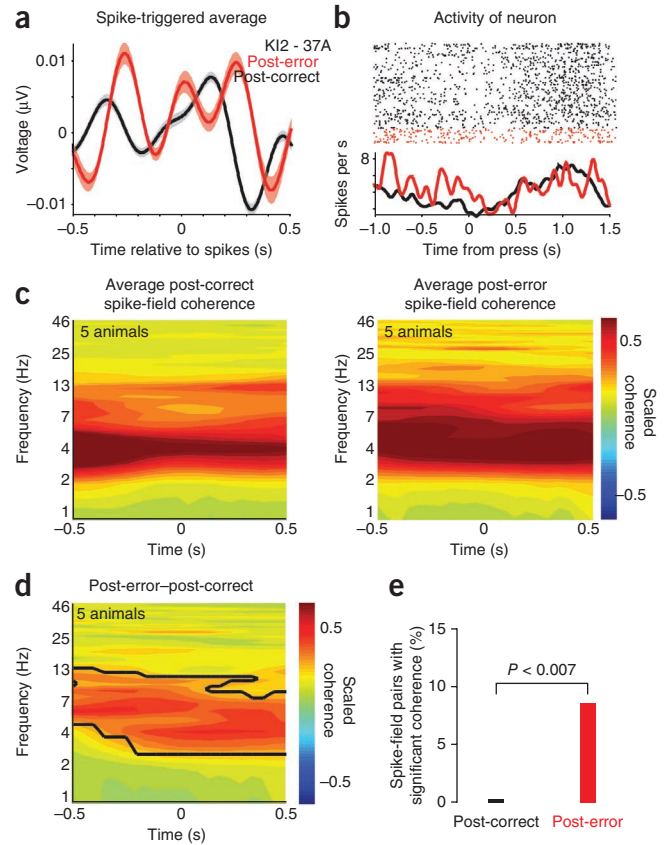


Figure 2 Time-frequency analysis revealing enhanced low-frequency power after errors. **(a)** In post-correct trials in humans, there was less low-frequency power than in post-error trials. **(b)** In post-correct trials in rodents, there was less low-frequency power than in post-error trials. **(c)** A direct comparison of post-error and post-correct trials in humans revealed stronger theta modulation to the imperative tone in post-error trials. **(d)** Trial-to-trial variation in low-frequency EEG signals in humans was significantly correlated with subsequent response latency (RL; electrode Cz). The current source density of the scalp topographies (bottom) revealed that these effects were prominent over the medial frontal regions. **(e)** Direct comparison of post-error and post-correct trials in rodents revealed markedly stronger low-frequency modulation to the imperative tone in post-error trials. **(f)** Trial-to-trial variation in 4–25 Hz frequencies in rodents was strongly correlated with subsequent response latency. In **d** and **f**, times were aligned to the target time, and black contours indicate significant differences determined by *t* test between post-error and post-correct trials ($P < 0.05$) or Spearman's (non-parametric) correlations ($P < 0.05$). **(g)** Midfrontal and motor sites in humans had significantly more low-frequency coherence in post-error compared to post-correct trials. **(h)** A similar pattern was observed in rodents between 12 MFC and 12 motor cortex (MC) channels in three rats. Times in **g** and **h** were aligned to the trial initiation, and black contours indicate significant differences determined by *t* test between post-error and post-correct trials ($P < 0.05$).

Figure 3 Medial frontal single neuron spiking is coupled with low-frequency oscillations. (a) Spike-triggered average of a medial frontal neuron for which local field potentials were averaged across all spikes within 2 s of the lever press for a single neuron. For this neuron, the spike-triggered average revealed robust low-frequency oscillations in post-error trials compared to post-correct trials; the shaded area represents the s.e.m. (b) Peri-event raster of the neuron in a revealing different patterns of activity after errors as well as low-frequency oscillations in firing rates. (c) Spike-field coherence in post-correct and post-error trials. (d) Post-error trials were characterized by enhanced low-frequency spike-field coupling. Times were aligned to the target time; black contours indicate significant differences determined by *t* test between post-error and post-correct trials ($P < 0.05$). (e) 9% of medial frontal neurons had significant low-frequency (below 12 Hz) spike-field coherence in post-error trials compared to no significant spike-field pairs in post-correct trials. The *P* values shown were calculated by a proportions test.



Spectral analysis of post-error signals

To investigate the spectral dynamics of post-error adjustments, we examined the time-frequency power spectra of human EEGs and rodent local field potentials (LFPs) in post-correct and post-error trials (Fig. 2a,b). This analysis directly compared the power spectra over time in post-error trials with the power spectra in post-correct trials. In humans, theta power (4–8 Hz) over the midfrontal leads was present in all trials (Fig. 2a) but was much stronger in post-error trials (Fig. 2c; $P < 0.05$). If theta power indicates a signal that is related to behavioral adjustment, then it may be expected to correlate with response-time adjustments. Indeed, we found that midfrontal theta-band power was more strongly correlated with response-time adjustments in post-error compared to post-correct trials (Fig. 2d). Topographic plots of current density revealed that these relationships occurred over the midfrontal sites, corresponding to generative sources from the MFC and recapitulating findings from previous humans studies²¹.

In rodents, time-frequency analysis also revealed strong low-frequency power in all trials (below 12 Hz; Fig. 2b). These frequencies were enhanced specifically in post-error compared to post-correct trials (Fig. 2e). As in humans, trial-to-trial power in the theta to beta ranges (Fig. 2f; 4–25 Hz) was more strongly correlated with response-time adjustments in post-error compared to post-correct trials. Taken together, these data suggest that humans and rodents share features of adaptive control through low-frequency oscillations in the MFC.

Interactions between the MFC and motor cortex

Adaptive control signals from the MFC must access the motor system to exert control over action. Synchronous field oscillations have been shown to entrain activity across distant brain regions^{22,23}, providing a candidate mechanism for top-down prefrontal control over the motor cortex^{8,10,21}. Neurons in the rodent motor cortex have been shown to encode variations in reaction-time performance^{24,25} and are influenced by top-down input from the MFC¹⁰. We used spectral coherence methods to examine interactions between the medial frontal and motor cortices in the time-estimation task. In humans, intersite phase coherence was significantly increased between the midfrontal leads and motor sites contralateral to the response hand in post-error as compared to post-correct trials (Fig. 2g). This difference between conditions was absent, and was even slightly reversed, when tested at an intermediary site (Supplementary Fig. 2), demonstrating that this effect was not due to volume conduction. In the rodent study, we simultaneously recorded 12 medial frontal fields and 12 motor cortex fields in three animals. As in the human study, intersite phase coherence was significantly increased in post-error

as compared to post-correct trials (Fig. 2h). Together our findings in the human and rat studies are consistent with previous findings suggesting that low-frequency oscillations act as a mechanism for entraining activity between the medial frontal and motor cortices in service of adaptive control of performance²⁶.

MFC neurons and fields are coherent after errors

Next we investigated whether the spike activity of neurons in the MFC was linked to the observed increase in low-frequency power after errors. Local field oscillations facilitate the rhythmic excitability of neurons and can create temporal windows for organizing functional ensembles of neurons^{23,27}. Spike-triggered averages of medial frontal field potentials revealed that spikes in post-error trials had robust low-frequency coupling when compared to spikes in post-correct trials (Fig. 3a). For many neurons, firing rates were elevated in post-error trials, and trial-averaged spike density functions exhibited temporal fluctuations (Fig. 3b). To examine the dynamics of this functional coupling, we used spike-field coherence²⁸ to analyze the relationships between 81 medial frontal neurons and 28 medial frontal field potentials simultaneously recorded from five animals. This type of analysis investigates trial-by-trial relationships of time-frequency coherence between single neuronal activity and the local field potential (Fig. 3c,d). We found that spike-field coherence was much stronger in post-error as compared to post-correct trials (Fig. 3d,e; there were no spike-field pairs with significant coherence in post-correct trials compared to seven pairs in post-error trials; $\chi^2 = 7.31$, $P < 0.007$), particularly between 2 and 13 Hz (Fig. 3d). These findings demonstrate that single medial frontal neurons can be entrained to low-frequency local field oscillations that are elevated in post-error trials.

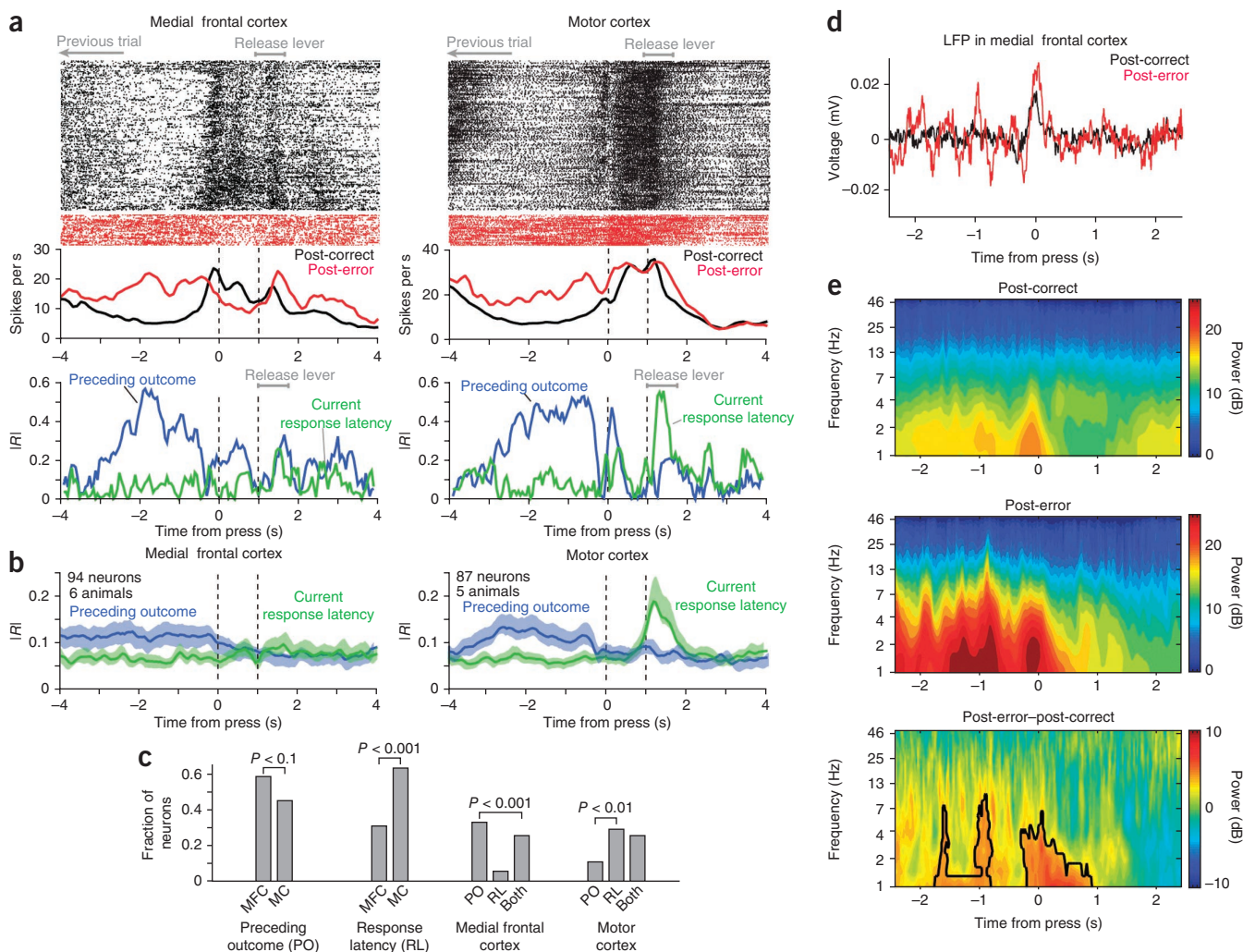


Figure 4 Encoding of previous outcomes in the medial frontal and motor cortices. **(a)** Examples of spike activity and correlation coefficients ($|R|$) from the partial correlation analysis are shown for neurons in the medial frontal and motor cortices. **(b)** Group summary for the sliding-window partial correlation analysis revealing that neurons in both cortical areas were sensitive to the previous outcome (blue) and that only neurons in the motor cortex were sensitive to variations in response latency (green). Error shading, s.e.m. **(c)** Fractions of neurons that were selective to previous outcome and current response latency and that were sensitive to either or both of these behavioral factors are summarized. Significance was assessed over all data windows (± 2 s around the press event) by a proportions test. **(d)** Spiking correlates of previous outcomes were accompanied by increased low-frequency oscillations in the field potential, as was apparent in the trial-averaged ERP and event-related spectral power. **(e)** The MFC local field potentials had prominent low-frequency modulation around the time of the response. The plots were aligned to the trial initiation time; black contours indicate significant differences determined by t test between post-error and post-error trials ($P < 0.05$)

MFC neurons encode adaptive control

To further explore the cellular basis of adaptive control, we investigated the spiking activity of single units from the rodent frontal cortex as a function of previous outcome using partial correlation analysis. We analyzed activity from 94 units from the MFC in six animals and 87 units from the motor cortex in five animals. We used partial correlation to measure the relationship between the firing rate of each neuron and two behavioral variables (prior outcome and current response latency). We measured prior outcome as the duration of the response in the previous trials, which was less than 1 s for premature responses. We carried out partial correlation analysis using the MATLAB function ‘partialcorr’ and measured correlation using Spearman’s rank correlation. By using partial correlation we were able to isolate effects of the prior outcome that were independent of the current response time and vice versa. To isolate the effects of each behavioral variable, the analysis fit a least-squares regression

model to explain the effects of one behavioral variable (for example, response times) on spike counts measured in a sliding data window around the task events. Then a second regression model was fit to explain the effects of the other behavioral variable (for example, previous outcome) on the residual variance (for example, due to response times). We used a 200-ms data window to measure firing rates and a step size of 50 ms.

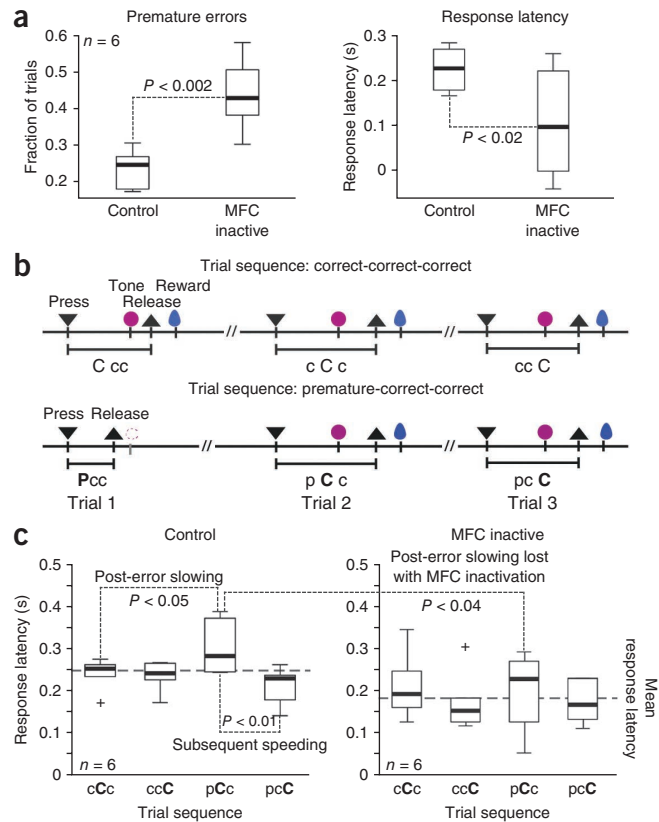
The partial correlation analysis revealed clear examples of neurons that varied with previous behavioral outcome in both the medial frontal and motor cortices (Fig. 4a). In both cortical areas there was a steady encoding of the previous behavioral outcome throughout the period before the trial (Fig. 4b). Neurons in the motor cortex, but not the MFC, later encoded the response latency in the current trial (Fig. 4b). Over the entire trial epoch (± 2 s around the lever press), slightly more neurons in the MFC were sensitive to the previous behavioral outcome ($\chi^2 = 2.86$, $P < 0.1$), and significantly

Figure 5 Loss of adaptive control after inactivation of the MFC.

(a) Reversible inactivation of the MFC in six rats increased the fraction of trials with premature responses and reduced the overall response times. Significant differences were determined by *t* test. (b) Given the erratic performance in the inactivation sessions with runs of premature errors, it was essential to confirm that effects on response latency adjustments would be found in controlled sequences of trials in which rats made two consecutive correct responses (C) after making either a correct response or premature error response (P). (c) Analysis of the trial sequences revealed clear evidence for slowing of response latencies after premature errors and a subsequent speeding in the control session (in which saline was infused into the MFC). This was not observed in sessions in which the MFC was inactivated. Inactivation of the MFC also led to an overall speeding of responses and eliminated the post-error slowing and subsequent speeding after the corrected response. In the box-and-whisker plots in a and c, the horizontal lines indicate the median, the boxes indicate the interquartile range, and the '+' indicate 1.5 times the interquartile range. Significant differences were determined by a *t* test.

more neurons in the motor cortex were sensitive to response latency ($\chi^2 = 17.75$, $P < 0.001$; Fig. 4c). However, as there was a clear sequential effect of previous behavioral outcome in this task, we examined the fractions of cells that were sensitive exclusively to both previous outcomes and response latency in the current trial. There was a clear difference in the encoding of these behavioral measures between the medial frontal and motor cortices (Fig. 4c). More neurons in the MFC encoded the previous behavioral outcome exclusively ($\chi^2 = 21.47$, $P < 0.001$). By contrast, more neurons in the motor cortex encoded response latency exclusively ($\chi^2 = 8.22$, $P < 0.01$).

These effects of prior outcomes were also apparent in local field potential recordings from the MFC. For example, ERPs synchronized to the start of the trial were larger in post-error trials compared to post-correct trials and clearly showed low-frequency rhythms in the pre-trial period (Fig. 4d; whereas the LFPs shown in Fig. 1c were time locked to the target time, here they were time locked to lever press). Spectral analysis revealed elevated low-frequency power (below 8 Hz) around the response in post-error trials (paired *t* test $t_5 = -4.23$, $P < 0.001$; Fig. 4e and Supplementary Fig. 3). Together these findings suggest that neuronal activity in the MFC encodes information that is involved in monitoring performance and could influence the control of response adjustments by the motor cortex.



MFC inactivation eliminates adaptive control

To test the causal and directional nature of the medial frontal control over the motor cortex, we recorded from the motor cortex while inactivating the MFC using muscimol²⁹, an approach that we have described in extensive detail previously^{10,11,29,30}. In six rats, inactivating the MFC resulted in more premature errors (paired *t* test $t_5 = -6.14$, $P < 0.002$) and reduced overall response latencies (paired *t* test $t_5 = 4.01$, $P < 0.02$; Fig. 5a). Overall behavioral performance was much more erratic in the inactivation sessions, which resulted in more consecutive premature errors and therefore complicated the analysis of sequential effects. Rats showed overall speeding of

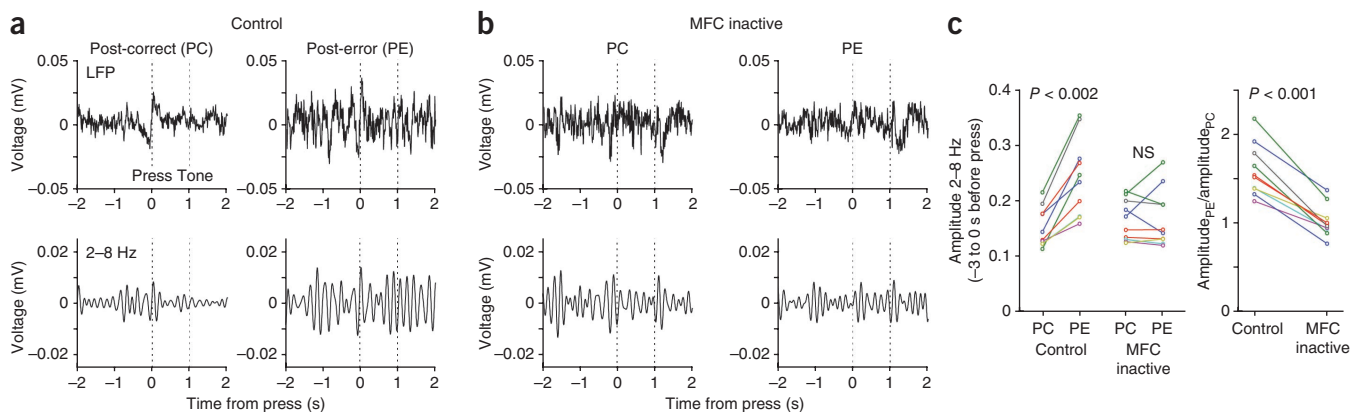
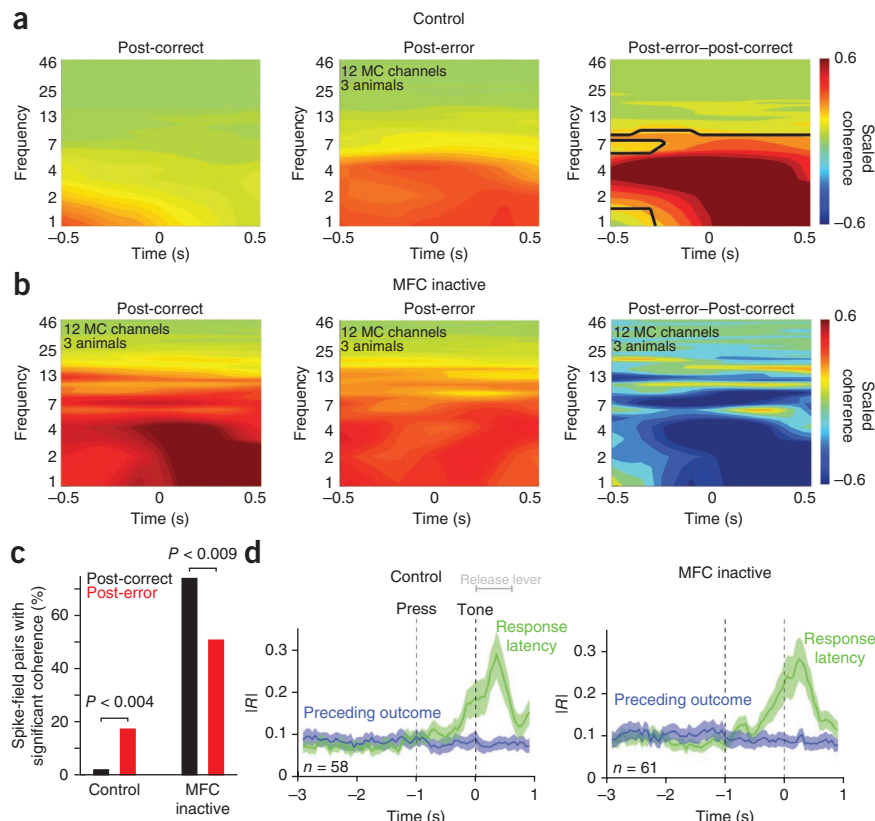


Figure 6 Inactivation of the MFC eliminated post-error increases in low-frequency oscillations in the motor cortex. (a) Peri-event averages of wideband field potentials (top) and bandpass-filtered signals (2–8 Hz; bottom) are shown from the motor cortex of one rat. In the control session, low-frequency oscillations were elevated in post-error trials. (b) Sessions in which the MFC was inactivated. (c) Z-transformed amplitude in the range between 2 and 8 Hz, as measured using the Hilbert transform. Medial inactivation caused low-frequency oscillations to become equivalent in the post-correct and post-error trials. This effect was found in every field potential examined from three rats. NS, not significant. Significant differences were determined by *t* test.

Figure 7 The rat MFC directly influences post-error low-frequency oscillations in the motor cortex in the service of adaptive control. **(a)** In control sessions, low-frequency spike-field coherence in the motor cortex in post-error trials was less prominent than in post-correct trials, as was apparent in comparisons of spike-field coherence between post-error and post-correct trials (right). Black contours indicate significant differences determined by *t* test between post-error and post-error trials ($P < 0.05$). **(b)** Medial frontal inactivation increased post-correct spike-field coherence and abolished differences between post-error and post-correct trials (right). **Supplementary Figure 5** shows comparisons between control and medial frontal inactivation sessions. **(c)** Medial frontal inactivation increased the numbers of neurons with significant spike-field coherence in post-correct trials. These data suggest that with medial frontal inactivation, low-frequency coherence is no longer specific to post-error trials; significant differences were determined by a proportions test. **(d)** Changes to spike-field coupling occurred in the absence of any effects of medial frontal inactivation on the sensitivity of the motor cortical neurons to prior behavioral outcome or response latency (the data shown are a subset of those in **Fig. 4** and have slightly less predictive power for previous outcome). Shaded areas, s.e.m.



response latencies in medial frontal inactivation sessions after making correct responses (median adjustment for the six rats in control sessions, -0.01 s; inactivation sessions, -0.180 s; paired *t* test $t = 2.77$, $P < 0.04$). To ensure that the behavioral effects of medial frontal inactivation were not due to the erratic performance in the inactivation sessions, we searched for sequences of trials in which the rats performed three consecutive correct responses or made a premature error and then made two consecutive correct responses (**Fig. 5b**). In the control sessions, there was clear evidence for post-error slowing (paired *t* test $t_5 = -2.58$, $P < 0.05$) and a subsequent post-correct speeding of performance after the next correct response (paired *t* test $t_5 = 3.86$, $P < 0.01$; **Fig. 5c**). Notably, in medial frontal inactivation sessions, rats showed an overall speeding of response latencies, and this eliminated both the post-error slowing and the subsequent post-correct speeding (**Fig. 5c**; all paired *t* tests with $P > 0.1$). Post-error response latencies were faster in inactivation sessions (paired *t* test $t_5 = 2.75$, $P < 0.04$; **Fig. 5c**), whereas post-correct response latencies were unchanged (paired *t* test $t_5 = 0.88$, $P < 0.42$).

In summary, these behavioral analyses establish that the MFC is crucial for the adaptive control of response times. In the absence of medial frontal function, rats show (i) an overall speeding of response times, (ii) an enhanced speeding of performance after correct responses and (iii) a loss of post-error adjustments. In the sections below, we investigate neural activity in the motor cortex in the absence of medial frontal control.

MFC inactivation eliminates motor cortex error activity

In three rats, we simultaneously inactivated the MFC while recording field potentials and single units in the motor cortex. Analysis of the field potentials from 19 channels across three animals revealed differential expression of low-frequency oscillations in post-error trials (**Fig. 6a**). Peri-event averages of bandpass-filtered (2–8 Hz)

LFPs showed a clear enhancement of oscillatory content in post-error trials (**Fig. 6a**), with a larger power envelope of the oscillations as derived by Hilbert transform (control sessions, paired *t* test $t_{18} = -3.62$, $P < 0.002$; inactivation sessions, paired *t* test $t_{18} = -0.19$, $P > 0.8$; ratio of inactivation to control, paired *t* test $t_{18} = 5.3$, $P < 0.001$; **Fig. 6b**). Surprisingly, these differential signals were eliminated when the MFC was inactivated (**Fig. 6a,b**). Spectral analysis of the motor cortex LFPs showed that medial frontal inactivation eliminated the power enhancement in post-error trials (**Fig. 6c** and **Supplementary Fig. 4**). Together these results suggest that low-frequency oscillations in the motor cortex were uncoupled from prior outcomes when the MFC was inactivated.

Motor cortex spike-field coherence requires the MFC

To examine how spike activity in the motor cortex was affected by medial frontal inactivation, we used spike-field coherence to examine spike activity from 58 neurons in the control sessions and 61 neurons in medial frontal inactivation sessions. Under control conditions, there was increased post-error spike-field coherence compared to in the post-correct trials (**Fig. 7a–c**; ten spike-field pairs with significant coherence in post-error trials compared to one pair in post-correct trials; $\chi^2 = 8.1$, $P < 0.004$). Similar to the LFP results (**Fig. 6a** and **Supplementary Fig. 4**), we observed strong spike-field coherence in post-correct trials (**Fig. 7c**; 45 spike-field pairs with significant coherence) and post-error trials (31 pairs, $\chi^2 = 6.8$, $P < 0.009$; different from control sessions, $\chi^2 = 20.5$, $P < 0.001$; **Supplementary Fig. 5**).

Although there were clear consequences of inactivating the MFC on spike-field coherence in the motor cortex, there was no effect on the basic firing properties of motor cortex neurons¹⁰. To investigate the predictive relationship of the motor cortex with response time and medial frontal inactivation, we used partial correlation (as in **Fig. 4**).

We found no effects of inactivation on the average correlation between firing rates and prior outcomes or current response latencies (Fig. 7d; these data are a subset of Fig. 4b) and no difference in the fractions of cells that exhibited significant correlations between firing rate and the two behavioral measures (firing rate, $\chi^2 = 0.56$, $P = 0.46$; prior outcomes, $\chi^2 = 0.35$, $P = 0.55$; current response latencies, $\chi^2 = 0.10$, $P = 0.75$). Therefore, our results suggest that the MFC achieves adaptive control over action by altering the coupling between spike activity and low-frequency oscillations, but not the firing rates of neurons, in the motor cortex.

In summary, these findings demonstrate that with the MFC inactivated, motor cortex spike-field coherence is no longer specific to post-error trials and is decoupled from variance in response latency (Supplementary Fig. 6). This result suggests that adaptive control of low-frequency coherence in the motor cortex requires medial frontal activity. These findings provide unique causal evidence for the idea that the MFC exerts adaptive control over the motor cortex and implicate low-frequency oscillatory coupling as a mechanism for realization and communication of the need for adaptive control across distant brain regions.

DISCUSSION

The findings reported here provide new evidence that low-frequency oscillations within the MFC (i) are increased after errors (Fig. 2b,e), (ii) predict adaptive control over response time (Fig. 2c,f), (iii) synchronize local neurons that contain information about the need for adaptive control (Figs. 3 and 4), (iv) are coherent with oscillations in the motor cortex that contain information about behavioral adaptation (Figs. 2g,h and 4) and (v) have a causal role in this process (Figs. 5–7). To the extent possible using noninvasive recordings, we demonstrated these same findings (i, ii and iv) in humans performing a highly similar task. Although prior work has shown medial frontal correlations between prior outcome and response time^{13,17} in humans and rodents, as well as coupling between local field potentials and single neurons²³, this is the first study, to our knowledge, to integrate these findings and demonstrate common mechanisms of behavioral adaptation in rodents and humans.

We found causal evidence for the role of medial frontal oscillations in adaptive control by reversibly inactivating the rat MFC using muscimol. Inactivating the MFC resulted in (i) a speeding of response times, especially after correct responses, (ii) a loss of behavioral adjustments after errors (Fig. 5c), (iii) an overall increase in low-frequency oscillations and loss of selective elevations in low-frequency power after errors (Fig. 6), (iv) a loss of the selective increase in phase locking between spikes and fields in the motor cortex in post-error trials (Fig. 7a,b) and (v) an overall increase in phase locking between spikes and fields (Fig. 7c). Notably, these effects occurred in the absence of changes in the firing-rate correlates of prior outcomes or response times in the motor cortex (Fig. 7d). These findings suggest that low-frequency oscillations facilitate synchronization among brain networks for representing and exerting adaptive control^{31–33}, including top-down regulation of behavior⁷, in the mammalian brain.

Previous studies^{11–13,21,32} in rats and humans have reported evidence for post-error changes in processing in the MFC. However, to our knowledge, this is the first direct comparison of rodent and human neural signals during the performance of a similar behavioral task and the first demonstration of common mechanisms for adaptive control in these two species. We report remarkably comparable ERPs and common low-frequency elements from microelectrodes in the rodent frontal cortex and human EEGs, suggesting that adaptive control is a conserved behavioral repertoire arising from the MFC³⁴.

Whereas rodents appeared to have broadband low-frequency power alterations that were related to adaptive control, humans had rather selective alterations within the theta band. It is notable that these species shared common features in their ERPs, in both correlation between low-frequency power and reaction time and coherence between prefrontal and motor regions. However, these comparisons were ultimately based on different signals, as the rat LFP arises from intracortical local-field potentials placed directly within layer II/III and the EEG leads are placed on the scalp some distance away from generative sources. Although scalp electrodes (in humans) and local microelectrodes (in rodents) certainly sample contributions from distinct anatomical areas, the concordance between these two signals is compelling and suggests a shared network for error-related adjustment.

It is encouraging to observe that errors are a common trigger of low-frequency oscillations, which are reliably correlated with performance adjustments. These results imply a common basis for behavioral adjustment after errors. However, brain networks differ vastly between humans and rodents. Furthermore, these species might use distinct behavioral strategies to perform this task. Future investigation of field potentials from depth electrodes in human intraoperative recordings and recordings in other animal models such as mice will shed light on the generality of these findings. Regardless, this conservation of functional neural resources facilitates an increasingly mechanistic understanding of human error processing using animal models. The development of such an animal model of adaptive control may provide tremendous benefit for the investigation of diseases that are characterized by impaired adaptive control, such as obsessive compulsive disorder⁷, depression³⁵, attention deficit hyperactivity disorder⁹, Parkinson's disease³³ and schizophrenia¹⁹, and for investigating dimensional aspects of these diseases, such as impulsivity and effortful control.

These findings lend support to the idea that low-frequency oscillations are the mechanism by which adaptive control is instantiated in prefrontal networks^{21,27}. Low-frequency oscillations, particularly in the theta band, have been seen commonly after humans make errors in a variety of contexts²¹. We found that low-frequency oscillations synchronize medial frontal neurons and that medial frontal neurons are correlated with and control low-frequency oscillations in the motor cortex at a trial-by-trial level. Notably, when the MFC was inactivated, low-frequency spike-field coherence in the motor cortex was more robust and was no longer specific to post-error trials. Thus, with the MFC inactivated, animals may function in a mode that is less flexible, and they may not benefit from information about previous outcomes. These findings not only suggest that prefrontal regions regulate the low-frequency coherence that is related to adaptive control in downstream areas such as motor cortex but also indicate that low-frequency coupling is required for behavioral adjustments after animals make errors. Our results support the idea that low-frequency oscillations are a candidate mechanism by which large populations of neurons can be synchronized across diverse brain regions in order to adjust behavior.

The medial frontal and motor areas reported here are not robustly connected³⁶. In rats, there are connections between the MFC and rostral part of the motor cortex (i.e., the rostral forelimb area), which could mediate adaptive control over action. The medial frontal and motor cortices may also share a thalamic relay to facilitate transient increases in phase consistency³⁷. Such phase-dependent coupling may synchronize multiple cortical and subcortical structures²³ and may originate from either synaptic activity within cortical layers or subcortical inputs, such as thalamic³⁷, monoaminergic³⁸ or cholinergic³⁹ projections. The circuit through which the MFC accesses the motor

cortex is unknown; however, the findings reported here establish that the low-frequency network dynamics of the motor cortex are regulated by activity in the MFC. Specifically, medial frontal inactivation eliminated post-error adjustments and abolished the specificity of low-frequency spike-field coupling in post-error trials.

The finding of generalized and enhanced motor spike-field coherence with medial frontal inactivation suggests the involvement of additional circuits that contribute to adaptive control. Future studies will need to record from cortical areas in combination with key structures such as the thalamus and subthalamic nucleus³³ to identify the full source and relay of adaptive control signals. Given that these low-frequency oscillations appear to be important for optimal behavioral performance, these efforts may illuminate pharmacological therapeutic opportunities that may benefit patients with impaired adaptive control.

In summary, we have detailed how low-frequency oscillations in the rodent MFC are modulated after errors and are coherent with single neurons across neural areas, providing a candidate mechanism for entraining functional networks in the service of behavioral control. Many of the core features of this system appear to be preserved in humans. This conserved neurobehavioral repertoire across mammalian species provides an appealing translational model for testing new pharmacological and stimulation techniques⁴⁰ that may contribute to the treatment of diseases with impaired adaptive control.

METHODS

Methods and any associated references are available in the [online version of the paper](#).

Note: Any Supplementary Information and Source Data files are available in the online version of the paper.

ACKNOWLEDGMENTS

We thank S. Masters for help with human data acquisition, N. Horst for technical editing and G.R. Yang for help with spike-field coherence code and simulations. This work was funded by National Institute of Neurological Disorders and Stroke grant K08 NS078100 to N.S.N., US National Institutes of Health (NIH) grant MH080066-01 and National Science Foundation (NSF) grant 1125788 to M.J.F., and NIH grant P01-AG030004-01A1 and NSF grant 1121147 to M.L.

AUTHOR CONTRIBUTIONS

N.S.N., J.F.C., M.J.F. and M.L. designed experiments and wrote the paper. N.S.N. and J.F.C. conducted experiments. N.S.N., J.F.C. and M.L. analyzed data.

COMPETING FINANCIAL INTERESTS

The authors declare no competing financial interests.

Reprints and permissions information is available online at <http://www.nature.com/reprints/index.html>.

- Bellman, R. & Kalaba, R. A mathematical theory of adaptive control processes. *Proc. Natl. Acad. Sci. USA* **45**, 1288–1290 (1959).
- Ridderinkhof, K.R., Ullsperger, M., Crone, E.A. & Nieuwenhuis, S. The role of the medial frontal cortex in cognitive control. *Science* **306**, 443–447 (2004).
- Holroyd, C.B. & Coles, M.G.H. The neural basis of human error processing: reinforcement learning, dopamine, and the error-related negativity. *Psychol. Rev.* **109**, 679–709 (2002).
- Rushworth, M.F.S. & Behrens, T.E.J. Choice, uncertainty and value in prefrontal and cingulate cortex. *Nat. Neurosci.* **11**, 389–397 (2008).
- van Meel, C.S., Heslenfeld, D.J., Oosterlaan, J. & Sergeant, J.A. Adaptive control deficits in attention-deficit/hyperactivity disorder (ADHD): the role of error processing. *Psychiatry Res.* **151**, 211–220 (2007).
- Velligan, D.I., Ritch, J.L., Sui, D., DiCocco, M. & Huntzinger, C.D. Frontal Systems Behavior Scale in schizophrenia: relationships with psychiatric symptomatology, cognition and adaptive function. *Psychiatry Res.* **113**, 227–236 (2002).
- Fitzgerald, K.D. *et al.* Error-related hyperactivity of the anterior cingulate cortex in obsessive-compulsive disorder. *Biol. Psychiatry* **57**, 287–294 (2005).
- Miller, E.K. & Cohen, J.D. An integrative theory of prefrontal cortex function. *Annu. Rev. Neurosci.* **24**, 167–202 (2001).
- Robbins, T.W. Shifting and stopping: fronto-striatal substrates, neurochemical modulation and clinical implications. *Phil. Trans. R. Soc. Lond. B* **362**, 917–932 (2007).
- Narayanan, N.S. & Laubach, M. Top-down control of motor cortex ensembles by dorsomedial prefrontal cortex. *Neuron* **52**, 921–931 (2006).
- Narayanan, N.S. & Laubach, M. Neuronal correlates of post-error slowing in the rat dorsomedial prefrontal cortex. *J. Neurophysiol.* **100**, 520–525 (2008).
- Carter, C.S. *et al.* Anterior cingulate cortex, error detection, and the online monitoring of performance. *Science* **280**, 747–749 (1998).
- Sheth, S.A. *et al.* Human dorsal anterior cingulate cortex neurons mediate ongoing behavioural adaptation. *Nature* **488**, 218–221 (2012).
- Rabbitt, P.M. Errors and error correction in choice-response tasks. *J. Exp. Psychol.* **71**, 264–272 (1966).
- Danielmeier, C. & Ullsperger, M. Post-error adjustments. *Front. Psychol.* **2**, 233 (2011).
- Dutilh, G. *et al.* Testing theories of post-error slowing. *Atten. Percept. Psychophys.* **74**, 454–465 (2012).
- Modirrousta, M. & Fellows, L.K. Dorsal medial prefrontal cortex plays a necessary role in rapid error prediction in humans. *J. Neurosci.* **28**, 14000–14005 (2008).
- Hampson, R.E. *et al.* Facilitation and restoration of cognitive function in primate prefrontal cortex by a neuroprosthesis that utilizes minicolumn-specific neural firing. *J. Neural Eng.* **9**, 056012 (2012).
- McClintock, S.M., Freitas, C., Oberman, L., Lisanby, S.H. & Pascual-Leone, A. Transcranial magnetic stimulation: a neuroscientific probe of cortical function in schizophrenia. *Biol. Psychiatry* **70**, 19–27 (2011).
- Kornblum, S. Simple reaction time as a race between signal detection and time estimation: a paradigm and a model. *Percept. Psychophys.* **13**, 108–112 (1973).
- Cavanagh, J.F., Cohen, M.X. & Allen, J.J.B. Prelude to and resolution of an error: EEG phase synchrony reveals cognitive control dynamics during action monitoring. *J. Neurosci.* **29**, 98–105 (2009).
- Buzsáki, G. *Rhythms of the Brain* (Oxford University Press, 2011).
- Fujisawa, S., Amarasingham, A., Harrison, M.T. & Buzsáki, G. Behavior-dependent short-term assembly dynamics in the medial prefrontal cortex. *Nat. Neurosci.* **11**, 823–833 (2008).
- Narayanan, N.S., Kimchi, E.Y. & Laubach, M. Redundancy and synergy of neuronal ensembles in motor cortex. *J. Neurosci.* **25**, 4207–4216 (2005).
- Laubach, M., Wessberg, J. & Nicolelis, M.A. Cortical ensemble activity increasingly predicts behaviour outcomes during learning of a motor task. *Nature* **405**, 567–571 (2000).
- Stefanics, G. *et al.* Phase entrainment of human delta oscillations can mediate the effects of expectation on reaction speed. *J. Neurosci.* **30**, 13578–13585 (2010).
- Womelsdorf, T., Johnston, K., Vinck, M. & Everling, S. Theta-activity in anterior cingulate cortex predicts task rules and their adjustments following errors. *Proc. Natl. Acad. Sci. USA* **107**, 5248–5253 (2010).
- Rosenberg, J.R., Amjad, A.M., Breeze, P., Brillinger, D.R. & Halliday, D.M. The Fourier approach to the identification of functional coupling between neuronal spike trains. *Prog. Biophys. Mol. Biol.* **53**, 1–31 (1989).
- Narayanan, N.S., Horst, N.K. & Laubach, M. Reversible inactivations of rat medial prefrontal cortex impair the ability to wait for a stimulus. *Neuroscience* **139**, 865–876 (2006).
- Allen, T.A. *et al.* Imaging the spread of reversible brain inactivations using fluorescent muscimol. *J. Neurosci. Methods* **171**, 30–38 (2008).
- von Stein, A., Chiang, C. & König, P. Top-down processing mediated by interareal synchronization. *Proc. Natl. Acad. Sci. USA* **97**, 14748–14753 (2000).
- Cavanagh, J.F., Zambrano-Vazquez, L. & Allen, J.J.B. Theta lingua franca: a common mid-frontal substrate for action monitoring processes. *Psychophysiology* **49**, 220–238 (2012).
- Cavanagh, J.F. *et al.* Subthalamic nucleus stimulation reverses mediofrontal influence over decision threshold. *Nat. Neurosci.* **14**, 1462–1467 (2011).
- Allman, J.M., Hakeem, A., Erwin, J.M., Nimchinsky, E. & Hof, P. The anterior cingulate cortex. The evolution of an interface between emotion and cognition. *Ann. NY Acad. Sci.* **935**, 107–117 (2001).
- Davidson, R.J., Pizzagalli, D., Nitschke, J.B. & Putnam, K. Depression: perspectives from affective neuroscience. *Annu. Rev. Psychol.* **53**, 545–574 (2002).
- Wise, S.P. Forward frontal fields: phylogeny and fundamental function. *Trends Neurosci.* **31**, 599–608 (2008).
- Vertes, R.P., Hoover, W.B., Do Valle, A.C., Sherman, A. & Rodriguez, J.J. Efferent projections of reuniens and rhomboid nuclei of the thalamus in the rat. *J. Comp. Neurol.* **499**, 768–796 (2006).
- Dzirasa, K. *et al.* Noradrenergic control of cortico-striato-thalamic and mesolimbic cross-structural synchrony. *J. Neurosci.* **30**, 6387–6397 (2010).
- Newman, E.L., Gupta, K., Climer, J.R., Monaghan, C.K. & Hasselmo, M.E. Cholinergic modulation of cognitive processing: insights drawn from computational models. *Front. Behav. Neurosci.* **6**, 24 (2012).
- Lee, T.G. & D'Esposito, M. The dynamic nature of top-down signals originating from prefrontal cortex: a combined fMRI-TMS study. *J. Neurosci.* **32**, 15458–15466 (2012).

ONLINE METHODS

Human EEGs. A total of 12 adults were recruited from the Brown University undergraduate subject pool and the Providence community to complete the experiment (six male; mean age = 21 years; s.d. = 2.22 years). All participants had normal or corrected-to-normal vision, no history of head trauma or seizures and were free from current psychoactive medication use. Data from one participant was excluded for having too few errors, yielding a final *n* of 11 participants. No statistical methods were used to predetermine sample sizes, but our sample sizes are similar to those reported in previous publications^{21,32,33,41}. Informed consent was obtained, and all procedures complied with the Institutional Review Board at Brown University.

Human time-estimation task. Participants were informed that they were expected to estimate a time period of 1.4 s. An irregular time interval was chosen to ameliorate the influence of simple counting for time estimation. Participants were also informed that in half of the trials, an imperative tone (MATLAB 'beep' command) would be played at the target time, and they were to respond as soon as possible in that instance. All trials began with a white fixation cross. After a varied inter-trial interval (ITI) (100–1,500 ms), the cross turned blue, indicating that participants could initiate the next trial. Participants began each trial by pressing the left joystick button; they then used the right button to signal their response. If they responded too early (errors) or too late (too slow), they received feedback indicating that they were 'incorrect' (for 1,000 ms, varied from 200–400 ms after the response) and had an additional post-error timeout of 2,000 ms. Unbeknownst to the participants, the response latency window varied using an adaptive algorithm that aimed to keep a 20% error rate (including error and too slow). Participants completed 500 trials total. Late and post-late responses were not analyzed.

EEG recording and preprocessing. EEGs were recorded using a 64-channel Brain Vision system. EEGs were recorded continuously with hardware filters set from 0.1 to 100 Hz, a sampling rate of 500 Hz and an online reference posterior to the vertex. Data windows for the continuous EEG recordings were placed around the onset of each trial (–1,500 to 6,000 ms). Data were then visually inspected to identify bad channels to be interpolated and bad epochs to be rejected. Eye blinks were removed using independent component analysis from EEGLab⁴². Data were then converted to current source density (CSD).

Rodents. Twelve Long-Evans male rats (aged 3–4 months) were trained to perform a delayed-response task. Of these rats, three had microwire arrays in the MFC only, three had microwire arrays in both the MFC and the primary motor cortex, and six had cannulae in the MFC and microwire arrays in the motor cortex. Of these latter six rats, only three had both well-isolated single units and local field potentials that were free of movement artifacts and line noise in the motor cortex. Rats were motivated by regulated access to water, whereas food was available *ad libitum*. Rats consumed 10–15 ml of water during each behavioral session, and additional water (5–10 ml) was provided 1–3 h after each behavioral session in the home cage. Single housing and a 12 h light, 12 h dark cycle was used; all experiments took place during the light cycle. Rats were maintained at ~90% of their free-access body weights during the course of these experiments and received 1 d of free access to water per week. The Animal Care and Use Committee at the John B. Pierce Laboratory approved all procedures. No statistical methods were used to predetermine sample sizes, but our sample sizes are similar to those reported in previous publications^{10,11,43}.

Task. Rats were trained to perform a time-estimation task using standard operant procedures²⁹ and motivation through regulated access to water. To perform this task correctly, animals had to press and hold a lever for a 1,000-ms delay period and release the lever promptly (within 600 ms) in order to receive a liquid reward (0.15 ml of water). The end of the delay period, or target time, was signaled by a 100-ms 72-dB 8-kHz tone. Response time was defined as the latency between the target time at the end of the delay period and lever release. In recording sessions, tones were omitted in 50% of trials (catch trials). If animals released the lever before the end of the 1,000-ms delay or after the 600-ms response window, the trials was scored as an error (premature or late, respectively), and all behavioral devices (pump, lever and houselight) were extinguished for a 4,000- to 8,000-ms ITI. No tones occurred in premature trials. Our previous work with this task in

rats suggested that catch trials do not affect prefrontal delay-related or task-related activity^{10,43} or behavior. As described previously^{10,43}, late trials were infrequent (<10% of trials) and were excluded from all rodent and human analysis.

Rodent behavioral apparatus. Operant chambers (MedAssociates, St. Albans, VT) were equipped with a lever, a drinking tube and a speaker driven to produce an 8-kHz tone at 72 dB using audio equipment from either Tucker-Davis Technologies (Alachua, FL) or manufactured in the instruments shop at the Pierce Laboratory. Behavioral arenas were housed in sound-attenuating chambers (MedAssociates). On correct responses, water was delivered by a pump (MedAssociates) connected to a standard metal drinking tube (AnCare) with Tygon tubing. Behavioral devices (houselight, pump and click stimulus) were activated after a delay of 100 ms after lever release. Response force was measured using a load cell (part #LCL-454G, Omega Engineering, Stamford, CT, rated to 0.454 N, or a thin film load cell, part #S100, Strain Measurement Devices, Meriden, CT, rated to 1 N) mounted at the back of the lever.

Medial frontal inactivation. Reversible inactivation of the MFC was performed according to procedures described previously²⁹. Briefly, 33-gauge cannulae (Plastics One) were implanted bilaterally into the dorsal prelimbic region (coordinates from bregma: anterior–posterior: +3.2, mediolateral ±1.4, dorsoventral –3.6 at 10° in the lateral plane) of three fully trained animals using aseptic surgical procedures. One week after surgery, animals were lightly anesthetized with halothane through a nosecone for 7 min and tested in the time-estimation task 45 min after recovery from anesthesia. On the first day of testing, 0.9% saline (Phoenix Scientific, St. Joseph, MO) was infused into the MFC (control sessions). On the second day of testing, muscimol¹⁰, a GABA_A receptor agonist (Sigma-Aldrich, St Louis, MO), was infused into the anterior cingulate cortex at 0.1 µg µl⁻¹ (inactivation sessions). On the third day of testing, animals were run without manipulation. Infusion was conducted by inserting injectors into the guide cannula, and 0.5 µl of infusion fluid was delivered per site at a rate of 15 µl per h (0.25 µl per min) with a syringe infusion pump (KDS Scientific, Holliston, MA). After injection was complete, the injector was left in place for 2 min to allow for diffusion. Rats were tested in the simple time-estimation task 45 min after the start of the infusions.

Neurophysiological recordings. Microelectrodes configured in 4 × 4 arrays of 50-µm stainless steel wires (250 µm between wires, impedance measured *in vitro* at 100–300 kΩ; Neurolinec, New York, NY) were implanted into the rat motor cortex (nine animals, six of which also had cannula in the prelimbic cortex; coordinates from bregma: anterior–posterior: –0.5, mediolateral: ±2.5–3.5, dorsoventral: –1.5 at –25° in the frontal plane; three had noise in their field potential and were excluded from LFP analyses) according to methods described in detail previously¹⁰. In six animals, microelectrode arrays were implanted targeting the dorsal prelimbic cortex in the MFC (three of these rats also had motor cortex recording electrodes; coordinates from bregma: anterior–posterior: +3.2, mediolateral: ±1.4, dorsoventral: –3.6 at 10° in the frontal plane; one rat had noise in its field potential and was excluded from LFP analyses; Fig. 1d). Once experiments were complete, rats were anesthetized and euthanized by injections of 100 mg per kg body weight sodium pentobarbital and were then transcardially perfused with either 10% formalin or 4% paraformaldehyde. Brains were sectioned on a freezing microtome, mounted on gelatin-subbed slides and stained for Nissl with thionin.

Neuronal ensemble recordings were made using a multi-electrode recording system (Plexon, Dallas, TX). Putative single neuronal units were identified online using an oscilloscope and audio monitor. The Plexon offline sorter was used to analyze the signals offline and remove artifacts. Spike activity was analyzed for all cells that fired at rates above 0.1 Hz. Statistical summaries were based on all recorded neurons. No subpopulations were selected or filtered out of the neuron database. Local field potential was recorded using wideband boards and was bandpass filtered between 0.07 and 8,000 Hz. Principal component analysis (PCA) and waveform shapes were used for spike sorting. Single units were identified as having (i) consistent waveform shape, (ii) separable clusters in PCA space, (iii) average estimated amplitude at least three times larger than background activity, (iv) a consistent refractory period of at least 2 ms in the interspike interval histograms and (v) consistent firing rates around behavioral events (as measured by a run test of firing rates across trials around behavioral events; neurons with $|z|$ scores >4 were considering 'nonstationary' and were

excluded). Analysis of neuronal activity and quantitative analysis of basic firing properties were carried out using Stranger (Biographics, Winston-Salem, NC), NeuroExplorer (Nex Technologies, Littleton, MA) and custom routines for MATLAB. Peri-event rasters and average histograms were constructed around lever release, lever press and tone offset.

Partial correlation analysis was used to explore the relationship of spiking activity to prior outcome and response time using Spearman's nonparametric rank correlation in MATLAB (function `PARTIALCORR`). This analysis partials out the influence of response time or prior outcome (i.e., if the previous trial was correct or premature) on spike counts using a sliding window starting ± 2 s before lever press. Statistical significance was assessed by shuffling trial orders 1,000 times, and effect size was quantified using the absolute value of Spearman's ρ statistic.

Time-frequency and statistical analyses. For both rats and humans, all post-error analyses were restricted to correct trials immediately after a premature error (occurring before the imperative stimulus was presented). Normality was tested using the Jarque-Bera goodness-of-fit test, and where appropriate, nonparametric displays and statistics were used. Time-frequency calculations were computed using custom-written MATLAB routines²¹. Time-frequency measures were computed by multiplying the fast Fourier transformed (FFT) power spectrum of single-trial EEG or LFP data with the FFT power spectrum of a set of complex Morlet wavelets (defined as a Gaussian-windowed complex sine wave:

$$e^{i2\pi ft} e^{-\frac{t^2}{2x\sigma^2}}$$

where t is time, f is frequency (which increased from 1 to 50 Hz in 50 logarithmically spaced steps) and defines the width (or 'cycles') of each frequency band, set according to $4/(2\pi f)$ and taking the inverse FFT, σ is the standard deviation, and x is the dependent variable. The end result of this process is identical to time-domain signal convolution and resulted in the following: (i) estimates of instantaneous power (the magnitude of the analytic signal), defined as $Z[t]$ (power time series: $p(t) = \text{real}[z(t)]^2 + \text{imag}[z(t)]^2$); and (ii) phase (the phase angle) defined as $\arctan(\text{imag}[z(t)]/\text{real}[z(t)])$. Each epoch was then cut in length surrounding the event of interest (-500 to $+500$ ms). Power was normalized by conversion to a decibel (dB) scale ($10 \times \log_{10}[\text{power}(t)/\text{power}(\text{baseline})]$), which allowed a direct comparison of effects across frequency bands. The baseline for each frequency consisted of the average power from -500 to -300 ms before the onset of each trial.

Intersite phase coherence was used to measure the consistency of phase values for a given frequency band across two different recording sites. Inter-site

phase coherence values vary from 0 to 1, where 0 indicates random phases at that time-frequency point between channels and 1 indicates identical phase values at that time-frequency point between channels. Spike-triggered averages were calculated by plotting the average field potential around post-error and post-correct spikes for each neuron and field. To look at the time-frequency component of interactions between individual spikes and the field potential, we applied spike-field coherence analysis using the Neurospec toolbox²⁸, in which multivariate Fourier analysis was used to extract phase locking among spike trains and local field potentials. As above, phase-locking coherence values varied from 0 to 1, where 0 indicates no coherence and 1 indicates perfect coherence. Fractional coherence was plotted by scaling the coherence by the power spectra. Statistical significance between conditions was determined by computing pixelwise paired-sample t tests between post-error and post-correct trials. For phase consistency, conditions were matched for epoch counts by response latency, matching post-error trials with post-correct trials.

For response latency analysis in medial frontal inactivation sessions (Fig. 5), comparisons were restricted to sequences of trials that were preceded by correct or premature responses. Response latencies could be negative because premature responses were included. Comparisons included 59 ± 10 (mean \pm s.e.m.) correct and 13 ± 1 error trials in the control sessions and 18 ± 12 correct and 16 ± 2 error trials in inactivation sessions.

Correlations between trial-by-trial EEGs or LFPs and response latency were computed within each condition for each participant separately using nonparametric Spearman's ρ values. Differences in trial-to-trial EEG or LFP response time patterns were investigated with paired-sample t tests of the sample ρ . We displayed the full time-frequency plots of human data for comparison with findings from the rats, but we had extremely strong regions of interest for the expected findings based on the underlying frequency in the human ERPs, the temporal-frequency effects in the rats and similar findings that have been explicitly detailed in our previous work²¹. In post-error trials, enhanced medial frontal activities were proposed to occur after the tone specifically in the theta (4–8 Hz) band, and response-locked correlations occurred with response times in a slightly lower and broader range⁴¹. Significant differences for spike-field coherence were computed from 95% confidence intervals and verified by bootstrapping time-shuffled data.

41. Cohen, M.X. & Cavanagh, J.F. Single-trial regression elucidates the role of prefrontal theta oscillations in response conflict. *Front. Psychol.* **2**, 30 (2011).
42. Delorme, A. & Makeig, S. EEGLAB: an open source toolbox for analysis of single-trial EEG dynamics including independent component analysis. *J. Neurosci. Methods* **134**, 9–21 (2004).
43. Narayanan, N.S. & Laubach, M. Delay activity in rodent frontal cortex during a simple reaction time task. *J. Neurophysiol.* **101**, 2859–2871 (2009).